Star formation history and the SED of galaxies: insights from resolved stars

Benjamin D. Johnson[1] and Daniel R. Weisz[2]

[1] UPMC-CNRS, UMR7095, Institut d'Astrophysique de Paris, F-75014, Paris, France

[2] Astronomy Department, University of Washington, Box 351580, Seattle, WA 98195-1580

email: `johnson@iap.fr`

Abstract. The star formation history (SFH) of galaxies is a principle uncertainty in SED modeling, and simple parameterizations of the SFH in typical SED fitting techniques may introduce biases in the resulting derived parameters. It is possible to constrain the SFH of galaxies more tightly through the observations of resolved stellar colour-magnitude diagrams with HST. This work is a first attempt to combine constraints on galaxy SFH from resolved stars with broadband SED modeling from the UV to the IR. This combination allows for the effects of different realistic SFHs on the SED to be quantified.

Keywords. galaxies:dwarf, galaxies:fundamental parameters

1. Introduction

Estimates of the stellar mass and star formation rate of galaxies from broadband SEDs rely on population synthesis models. An important ingredient of these models is the star formation history (SFH). The simplest models assume a constant SFR, for example to derive linear scalings between SFR and luminosity (e.g., Madau *et al.* 1998, Kennicutt 1998). More sophisticated modeling involves allowing the SFR to vary with time, though it is usually parameterized to be smoothly varying (e.g. τ-models with exponentially declining SFR). The parameterized SFH is then constrained by the SED of individual galaxies. Difficulties in this approach arise from 1) degenerecies between SFH and dust attenuation and stellar metallicity and 2) biases due to SFH that deviate from the assumed parameterization (e.g. with a different long-term SFR evolution or variable SFR on short timescales).

Stronger constraints on the SFH of nearby galaxies come from analysis of the colour-magnitude diagram (CMD) of resolved stars. Using HST these can be obtained for galaxies outside the local group. With such data it is possible to determine the effects of observationally constrained SFHs on measures of SFR and stellar mass that typically assume a smooth SFH. It is also possible to compare the SED expected given the SFH to the observed SED, both to constrain the effects of other galaxy properties on the SED and to assess the performance of SED models in the ultraviolet (UV) and near-infrared (NIR).

2. The Effects of Realistic SFH on the SED

The sample of galaxies that we consider is drawn from the ANGST survey (Dalcanton *et al.* 2009). Galaxies in this survey have been observed in multiple bands with either the WFPC2 or ACS instrument onboard HST. Their small distances (< 4 Mpc) insure that individual stars can be detected to several magnitudes below the tip of the red giant branch. The distance limit also results in a sample that is dominated by dwarf galaxies

(median $M_* \sim 10^{7.4}$ $M_\odot$), mostly of later morphological type, but including some dwarf spheroidals. The sample generally has low metallicity and low dust attenuation.

The construction of CMDs and the method for determining the SFH from the CMD is described in Weisz *et al.* 2011 and references therein. Briefly, linear combinations of colour magnitude diagrams for SSPs with different ages are combined to fit the observed CMD, and the combination coefficients are used to construct the SFH. The time binning of the recovered SFH that we use is $\Delta \log t = 0.1$. An example SFH is shown in Figure 1.
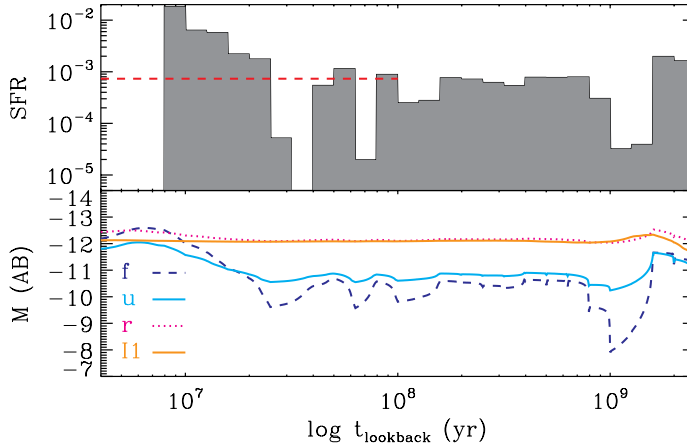

Figure 1. *Top:* Example SFH for UGC8091, inferred from the colour-magnitude diagram of resolved stars. The dashed line indicates $\langle SFR \rangle_8$ *Bottom:* Resulting evolution of the luminosity in several broad bands.

We can use the SFH derived from resolved stars as input for population synthesis codes. This allows the prediction of the SED in any bands at any lookback time. For this study we have used the FSPS v2.1 code of Conroy *et al.* (2009) with $0.2Z_\odot$ metallicity. This population synthesis code uses stellar evolutionary tracks that are consistent with those used for the derivation of the SFH from the CMDs, and we have been careful to use consistent stellar initial mass functions (IMF). We obtain very similar results using the population synthesis code of Bruzual (2007). The input SFH is also used to derive the SFR averaged over 100 Myr.

With the input SFH and the predicted FUV luminosity, we then construct the modeled SFR conversion factor

$$\epsilon_{FUV,8} = \nu L_{\nu,FUV} / \langle SFR \rangle_8$$

where $\nu L_{\nu,FUV}$ is the predicted far-UV luminosity (here in the *GALEX* FUV band) and $\langle SFR \rangle_8$ is the input SFR averaged over the last 100 Myr. This timescale is typically assumed to be the timescale probed by the far-UV ($\lambda \sim 1300 - 1800\text{Å}$), as this is the approximate lifetime of stars that dominate the far-UV luminosity of a population. This conversion factor is shown in Figure 2 as a function of several colours. We also show the conversion factor of Kennicutt (1998) (for the IMF used here) and that obtained for several exponentially declining models with different decline rates. We have ignored the effects of dust attenuation and metallicity variations. The important thing to note is the significant scatter in the SFR conversion factor at a given colour, much larger than predicted for different τ-models. The rms dispersion is a factor of two for this sample, and the range of $\epsilon_{FUV,8}$ is more than an order of magnitude. Furthermore, the scatter is

not well correlated with UV/optical colour. For some redder galaxies a large fraction of the UV luminosity appears to be contributed by stars older than 100 Myr.
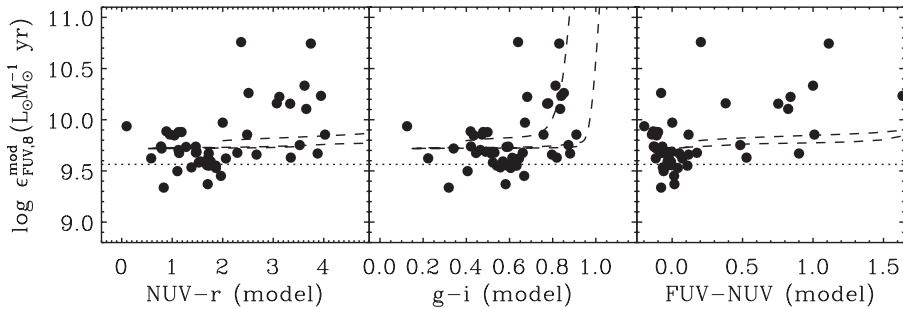

Figure 2. Conversion between SFR and FUV luminosity, as inferred from the SFH. The conversion factors are shown as a function of several colours. The dotted line shows the conversion factor of Kennicutt (1998), while the dashed lines show the expectations for several exponentially declining models.

3. Comparison to Observations

Observations of the sample include broadband photometry from *GALEX*, SDSS, and *Spitzer* Dale *et al.* (2009), Lee *et al.* (2011). Comparison of the predicted luminosties described above to the observed luminosities yields excellent agreement in the *g* or *B* band, expected since the resolved stars constitute a significant fraction of the total optical flux. In Figure 3 we compare observed UV colours to the colours predicted given the SFH. This shows that the observed UV and UV/optical colours are much redder than the prediction; observed galaxies are fainter in the UV (and have redder UV colours) than expected. The average offset is ~ 1 mag in the FUV and ~ 0.6 mag in the NUV.
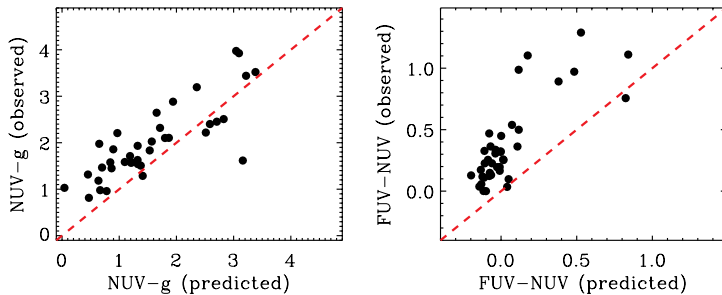

Figure 3. Comparison of observed UV/optical colours to the colours predicted given the SFH. The dashed line indicates perfect agreement. The observed colours are systematically redder in both NUV-g (*left*) and FUV-NUV (*right*).

One obvious possible cause for such dimming and reddening is dust attenuation. Estimates of dust attenuation are available from the ratio of $24\mu m$ *Spitzer* fluxes to the FUV fluxes, following Hao *et al.* (2011). As the sample consists largely of low mass galaxies, the metallicity and dust content is typically very small ($A_{FUV} < 0.35$ mag). Figure 4 shows that the inferred dust attenuation is lower than required to explain the observed

UV faintness of the sample galaxies relative to the predictions. Similar tests suggest that metallicity effects and stochastic star formation cannot explain the differences in the UV. Other possibilities include systematic errors in the determination of the recent SFH, or deficiencies in the modeling of the UV in the population synthesis models.
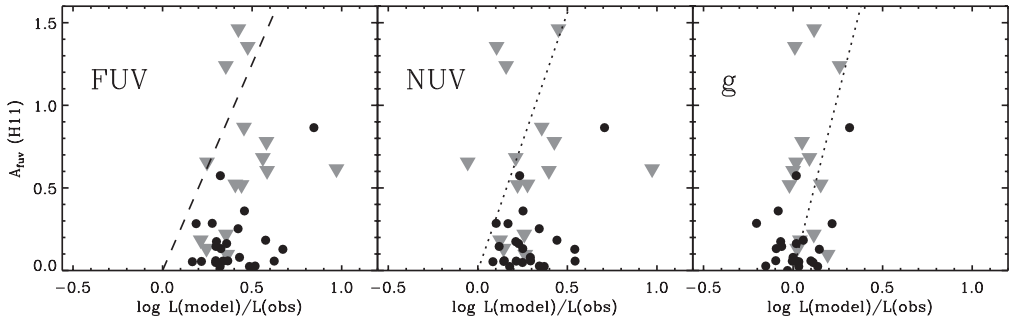

Figure 4. Dust attenuation. The FUV dust attenuation inferred from the 24μm to UV ratio is plotted against the ratio of the predicted luminosity to the observed luminosity. Gray triangles indicate upper limits to A_{FUV}. The attenuation required to explain any difference is shown as the dashed line. In the FUV and NUV bands the measured dust attenuation is always below this line and there is no correlation.

The model predictions in the *Spitzer* IRAC bands are sensitive to the treatment of TP-AGB stars. The predictions of models that include the unmodified isochrones of Marigo *et al.* (2008) are brighter than the observed $3.6\,\mu$m and $4.5\,\mu$m luminosities by 0.5 mag on average. A modification of the TP-AGB isochrones as suggested by Conroy *et al.* (2009) results in no average offset.

4. Conclusions

We have made a first step towards combining constraints from resolved stars with the broadband SED of galaxies. We have shown that it is possible to gain insight into the effects of observationally constrained SFHs on the conversion between SFR and UV luminosity. Effects on measures of stellar mass will be explored in a future work. We highlight an apparent discrepency between the observed UV luminosities and those expected given the SFH. We suggest that future work to simultaneously fit both the resolved stellar populations and the UV through NIR broadband SED may improve constraints on the SFH of nearby galaxies and provide a test of population synthesis models.

References

Bruzual, A. G. 2007, in *IAU Symposium*, Vol. 241, IAU Symposium, ed. A. Vazdekis & R. F. Peletier, 125
Conroy, C., Gunn, J. E., & White, M. 2009, *ApJ*, 699, 486
Dalcanton, J. J., Williams, B. F., Seth, A. C., *et al.* 2009, *ApJS*, 183, 67
Dale, D. A., Cohen, S. A., Johnson, L. C., *et al.* 2009, *ApJ*, 703, 517
Hao, C.-N., Kennicutt, R. C., Johnson, B. D., *et al.* 2011, *ApJ*, 741, 124
Kennicutt, R. C. 1998, *ARAA*, 36, 189
Lee, J. C., Gil de Paz, A., Kennicutt, Jr., R. C., *et al.* 2011, *ApJS*, 192, 6
Madau, P., Pozzetti, L., & Dickinson, M. 1998, *ApJ*, 498, 106
Marigo, P., Girardi, L., Bressan, A., *et al.* 2008, *A&A*, 482, 883
Weisz, D. R., Dalcanton, J. J., Williams, B. F., *et al.* 2011, *ApJ*, 739, 5